Journal of Peptide Science
J. Pept. Sci. 2008; **14**: 1183–1194
Published online 6 August 2008 in Wiley InterScience (www.interscience.wiley.com). DOI: 10.1002/psc.1057

JOURNAL OF PEPTIDE SCIENCE

Description of the low-affinity interaction between nociceptin and the second extracellular loop of its receptor by fluorescence and NMR spectroscopies

BRUNO VINCENT,[a,b] LIONEL MOULEDOUS,[a,b] BRICE BES,[a,b] HONORE MAZARGUIL,[a,b] JEAN-CLAUDE MEUNIER,[a,b] ALAIN MILON[a,b]* and PASCAL DEMANGE[a,b]*

[a] Université de Toulouse, Institute of Pharmacology and Structural Biology, IPBS, UPS, 31077, Toulouse, France
[b] CNRS, UMR 5089, IPBS, Toulouse, France

Received 7 March 2008; Revised 15 May 2008; Accepted 26 May 2008

Abstract: The second extracellular loop (ECL2) of the Noc receptor has been proposed to be involved in ligand binding and selectivity. The interaction of Noc with a constrained cyclic synthetic peptide, mimicking the ECL2, has been studied using fluorescence and NMR spectroscopies. Selective binding was shown with a dissociation constant of ~10 μM (observed with the constrained cyclic loop and not with the open chain), and residues involved in ligand binding and selectivity have been identified. This bimolecular complex is stabilized by (i) ionic interactions between the two Noc basic motives and the ECL2 acidic residues; (ii) hydrophobic contacts involving Noc FGGF *N*-terminal sequence and an ECL2 tryptophane residue. Our data confirm that Noc receptor's ECL2 contributes actively to ligand binding and selectivity by providing the peptidic ligand with a low affinity-binding site. Copyright © 2008 European Peptide Society and John Wiley & Sons, Ltd.

Keywords: GPCR; nociceptin; dynorphin; opioid receptors; extracellular loop; NMR spectroscopy; neuropeptides; membrane receptors

INTRODUCTION

The Noc/orphanin FQ receptor (NOP) regulates pain perception either directly or by modulation of the opioid system, as well as stress and anxiety, food intake, and drug dependence [1,2]. All these physiological properties make it an interesting drug target and justify investigation about the way Noc binds and activates its receptor. The NOP receptor belongs to the large family of GPCRs which share a common topology consisting of an *N*-terminal extracellular region, a *C*-terminal intracellular tail, and seven transmembrane helices connected by three extracellular and intracellular loops. It is closely related to opioid receptors and its endogenous ligand is a 17-amino acid peptide whose sequence is FGGFTGARKSARKLANQ [3]. Signal transduction is achieved by conformational modifications of the receptor after ligand binding, which finally trigger modifications in intracellular receptor–G protein interactions. Similarly to many peptides binding GPCRs, Noc is thought to interact with its receptor at the level of both transmembrane and extracellular domains [4,5]. Similar to opioid receptors, the extracellular loops were assumed to play a role both in ligand binding and in ligand selectivity [6].

The study of GPCR structure and activation mechanism is made difficult by the fact that they are large transmembrane proteins. To date, only two GPCR structures have been resolved by crystallographic studies: the bovine rhodopsin [7] and the human β2 adrenergic receptors [8,9]. This was made possible by the ability to isolate large quantities of pure receptor from its native membrane environment or overexpression in heterologous cell lines [10]. An alternative approach to X-ray structure determination of entire GPCRs is to study the interaction between chosen fragments of GPCR by liquid-state NMR [11]. The validity of this strategy can be illustrated by a study that showed good agreement between high-resolution NMR structures of peptides corresponding to loops of bacteriorhodopsin and the X-ray structure of the full size protein [12]. Since then, the fragment approach was successfully applied to the study of GPCR loops, either alone [13–16] or in interaction with ligands [17–23]. The NMR approach is able to provide information about intermolecular interactions between loops and ligands even for disordered flexible regions of the peptides. Since Noc is known to be highly flexible in aqueous solution [24], we have decided to use a fragment approach to analyze the dynamics of its interaction with its receptor.

Abbreviations: CD, circular dichroism; DOP1 receptor, human δ opioid receptor, Dyn, dynorphin; ECL2, extracellular loop II, cyclic peptide; GPCR, G protein coupled receptor; HSQC, heteronuclear single quantum correlation; KOP1 receptor, human κ opioid receptor; MS, mass spectrometry; NMR, nuclear magnetic resonance; NOE, nuclear Overhauser effect; NOESY, nuclear Overhauser enhancement spectroscopy; Noc, nociceptin; NOP receptor, nociceptin/orphanin FQ receptor; MOP1 receptor, human μ opioid receptor; TCEP, tris(2-carboxyethyl) phosphine hydrochloride; TFA, trifluoroacetic acid; TOCSY, total-correlation spectroscopy.

*Correspondence to: Alain Milon, CNRS, UMR 5089, IPBS, Toulouse, France; e-mail: Alain.milon@ipbs.fr
Pascal Demange, Université de Toulouse, Institute of Pharmacology and Structural Biology, IPBS, UPS, 205 route de Narbonne, 31077, Toulouse, France; e-mail: Pascal.Demange@ipbs.fr

The NOP receptor shares a high-sequence similarity with the three classical opioid receptors, μ, δ, and κ [3]. However, NOP is not assimilated to a classical opioid receptor since it does not bind endogenous opioid peptides. The main differences in primary sequence are located in the extramembrane domains (*N*- and *C*-terminal tails and extracellular loops ECL1, ECL2, ECL3). Among these variable parts, ECL2 is thought to play a critical role in Noc binding and receptor activation. Originally, it was the acidic nature of the NOP receptor ECL2 that prompted Meunier *et al.* to search for a basic peptide as the endogenous ligand for their orphan receptor [25]. Within the opioid receptor family, only the κ (KOP) receptor and its endogenous ligand, Dyn, present the same acidic/basic feature but the interaction between the two ligands and their respective receptors appears to be different. The study of NOP/KOP receptor chimeras showed that introducing the ECL2 of NOP in the chimeras was mandatory in order to restore a full response to Noc while the response to Dyn was unaffected [26]. Moreover, structure/activity relationship studies of the two ligands showed that the integrity of the central basic part of Noc was of primordial importance for its biological activity [27,28]. On the contrary, Dyn can be truncated down to its (1–7) *N*-terminal fragment without losing its pharmacological properties [29,30]. Finally, a photo affinity labeling study coupled to molecular modeling confirmed that Noc interacts with the extracellular loops of the receptor [31]. Several studies have already pointed out the implication of ECL2 for the activation of other GPCR. Site-directed mutagenesis of ECL2 residues triggers constitutive activation of the C5a receptor [32], confers agonist properties to an antagonist of the GnRH receptor [33], and induces an increase of EC_{50} for VPAC2 ligands [34]. Recently, a CD study of purified serotonin 5-HT4a receptors demonstrated that receptor activation leads to a conformational change of ECL2 [35].

All these data prompted us to characterize at a molecular level the determinants of Noc–ECL2 specific interaction. A cyclized ECL2 synthetic peptide was used in order to mimic the restrains induced by the transmembrane helices packing in the native protein, a strategy which has already been successfully applied to similar receptors [15,16]. Although previous work have reported the use of DPC micelles [14] and other membrane-mimetic media [20], we have chosen to study the Noc–ECL2 interaction in aqueous solution, and thus to deal with highly dynamical systems, assuming that this best represents the interfacial interactions occurring *in vivo*. Our results will be discussed in terms of amino acid selectivity occurring during this interaction, and we will show that although our system only represents a part of the ligand–receptor recognition, it reveals important aspects of this interaction.

MATERIAL AND METHODS

Synthesis and Peptide Purification

To mimic the ECL2 of the NOP receptor, a peptide of 26 amino acids (residues 189–214 of human NOP receptor) with two supplementary homocysteines at both ends was synthesized by using the standard Fmoc solid phase strategy on Wang resin. The cysteine 200 was mutated to a serine to avoid any cross-reaction during the disulfide bond formation. The peptide was purified by using RP-HPLC with a 0.01% TFA–acetonitrile gradient. An oxidation reaction for cyclization of the peptide by forming a homocystine was performed by solubilization in DMSO/H_2O (5% v/v) in the presence of 0.1% hydroxylamine to avoid the thiolactone formation under acidic condition. The formation of the disulfide bond between the two homocysteines at both ends was followed by HPLC chromatography (data not shown). In order to prepare the linear version of the peptide, the disulfide bridge of the cyclic EC2 loop between the two homocysteines was reduced by addition of TCEP in a molar ratio (ECL2/TCEP) 1 : 4.

Noc and ^{15}N specific labeled Noc were obtained by using the same peptide synthesis methods as described above. All these peptides were characterized by electron spray MS using a quadrupolar detection and the molecular masses confirmed the desired structures.

Fluorescence Spectroscopy

The fluorescence property of the unique ECL2 tryptophan was used to monitor the interaction between Noc and the constrained ECL2 peptide. Fluorescence spectra of ECL2 at a concentration of 10 μM in phosphate buffer pH 7.2 were recorded with an excitation wavelength of 285 nm. The fluorescence spectrum of Noc alone was subtracted during the binding experiment.

Single-site binding of Noc to the ECL2 was fitted to the following equation:

$$F_{obs} - F_0 = (F_f - F_0)\,(K_d + [L_t] + [P_t] - \sqrt{(K_d + [L_t] + [P_t])^2 - 4[L_t][P_t]}\,)/(2[P_t]) \quad (1)$$

where F_{obs} is the fluorescence intensities observed during addition of Noc; F_0, the initial ECL2 fluorescence; and F_f, the final fluorescence measured after saturation of all binding sites. P_t is the total ECL2 concentration and L_t is the Noc concentration. The K_d and final fluorescence values were fitted based on stochastic algorithms, using simulated annealing (GOSA, Biolog SA, France).

NMR Sample Preparation

Lyophilized peptides were dissolved in 10 mM Na_2HPO_4 phosphate buffer, at pH = 6, with 10% D_2O in H_2O. Concentrations of 2 mM and 100 μM were used for the assignment and titration experiments, respectively. Freshly prepared samples were used in each set of experiments.

NMR Experiments

NMR spectra were acquired on 600 MHz cryoprobe and 700 MHz TXI probe, Avance Bruker NMR spectrometers, at

DOI: 10.1002/psc

288 K. TOCSY and NOESY spectra were recorded in phase-sensitive mode and water suppression was achieved using a Watergate [36] or an excitation sculpting [37] pulse sequences. NOESY spectra were recorded with a mixing time of 300 ms and TOCSY spectra with a mixing time of 90 ms applied during the DIPSI spinlock sequence [38]. The typical spectral widths were 10 500 Hz in both dimensions, with 4096 data points in t_2 and 512 data points in t_1 and 32 to 160 scans.

The [^{1}H–^{13}C] and [^{1}H–^{15}N] HSQC experiments were recorded with a spectral width of 33 451 and 2258 Hz for ^{13}C and ^{15}N respectively and 10 500 Hz for ^{1}H. Spectra were recorded with 2048 data points in t_2 and 256 data points in t_1. Eighty scans were used for natural abundance ^{13}C spectra and eight scans for ^{15}N-labeled Noc. NMR data sets were processed using the Linux version of NMRPipe [39] with a shifted cosine-bell apodization in both dimension, and zero-filled to 4096 × 4096 complex points before Fourier transform. Data analyses were done using Sparky (Sparky 3, University of California, San Francisco).

Binding Experiment followed by NMR

The binding experiments were realized at 100 μM ECL2 concentration in a 10-mM pH 6 phosphate buffer. The peptide ratio (ECL2/Noc) was determined by integrating specific resonances on the 1D spectrum, i.e W_{24} HZ2 and Y_{23} HD protons of ECL2 and aromatic protons of Noc F_1 and F_4. Ten different ECL2/Noc ratios ranging from 0 to 1.5 were used. A relaxation delay of 3 s was used to ensure the full T_1 relaxation.

The dissociation constant K_d was determined by NMR assuming a 1 : 1 stoichiometry of the Noc–ECL2 complex. Since the rate of Noc–ECL2 complex dissociation is faster than the chemical shift separation, a single resonance was observed corresponding to the proportion of free and bound states.

The dissociation constants (K_d) for binding of Noc to its ECL2 were determined from the concentration dependence of ^{1}H and ^{15}N chemical shift changes in this fast exchange regime approximation.

^{15}N Relaxation Experiments

^{15}N longitudinal relaxation times, T_1, ^{15}N spin-lattice relaxation times, T_2 and ^{1}H–^{15}N steady-state NOEs were determined at 700 MHz as described in Ref. 40. The relaxation delays T for T_1 experiments were: 0.010, 0.050, 0.100, 0.200, 0.400, 0.600, 0.800, 1 s and for T_2: 0.017, 0.034, 0.086, 0.190, 0.397, 0.587, 0.794, 0.985, and 1.190 s. Values of steady-state heteronuclear ^{1}H–^{15}N NOE were determined from the ratios of the peak volumes with and without proton saturation, NOE = Isat/Iunsat. Relaxation time measurements (T_1, T_2) and ^{1}H–^{15}N NOE of Noc in complex with ECL2 were also carried out after addition of Dyn (1–17 aas) to the preformed ECL2/Noc (1/1) complex from a stock solution at 20 mM. The ECL2–Noc complex concentration used was 200 μM and Dyn was added to obtain Dyn/Noc ratio ranging from 0 to 43. The ratios were determined by integrating peaks corresponding to the HE protons of Dyn Y_1 and previously cited peaks of ECL2.

RESULTS

A Model for Noc–ECL2 Interaction Based on Synthetic Peptides

In order to study the interaction between Noc and ECL2 of its receptor (Figure 1(a)), we synthesized several peptides: Noc, a neuropeptide constituted of 17 amino acids (Figure 1(d)) and a cyclized peptide mimicking the extracellular loop of the NOP receptor (Figure 1(b)). Along the Noc sequence, six ^{15}N labeled amino acids were incorporated (Figure 1(d)) to probe the Noc–ECL2 complex and its dynamics. ECL2 of NOP receptor is well conserved in all species and differs from the other human opioid receptors (MOP1, DOP1, KOP1). A peptide sequence of the 26 amino acids corresponding to ECL2 was synthesized supplemented at both ends by a homocysteine. The intramolecular oxidation of homocysteines realized in DMSO, allowed us to obtain a cyclic constrained peptide where the *N*- and *C*-terminal distance is in the range of 8–12 ´Å, corresponding to the distance between the helices 4 and 5 in a published NOP receptor model [5]. The cyclic form of the peptide was confirmed by a peak on MS spectra corresponding to the $[M + H]^+$ at 3134.4 a.m.u. i.e. two mass units less than the reduced, open, linear form.

Fluorescence Spectroscopy of Noc–ECL2 Interaction

The cyclized ECL2 contains only one tryptophan (W_{211}) adjacent to a tyrosine (Y_{210}) which was used as an intrinsic probe to follow Noc–ECL2 interaction. Since the emission spectrum of this amino acid is highly sensitive to the solvent polarity, it can reveal information about its environment, conformational changes and/or direct interaction with a substrate [41]. The tryptophan emission spectrum of ECL2 has a maximum emission wavelength of 356 nm corresponding to water-exposed tryptophan residues [41]. Upon addition of Noc, a significant quenching was observed with no shift in the emission maximum. The binding curve (Figure 2) showed that the fluorescence intensity at 356 nm decreased in a saturation-dependent manner upon Noc addition. By fitting the data with the equations described in the Section on Material and Methods, we obtained a K_d value of 7.2 ± 3.5 μM. This fluorescence-quenching phenomena may occur by a specific interaction between one of the two phenylalanines present in the Noc and the ECL2 tryptophan, as was observed previously in cyclic hexapeptides [42].

^{15}N and ^{1}H Chemical Shift Perturbation upon Noc–ECL2 Interaction

^{15}N labeled Noc was synthesized in order to follow the influence of ECL2 interactions on chemical shifts and ^{15}N relaxation parameters. Specific labels were

DOI: 10.1002/psc

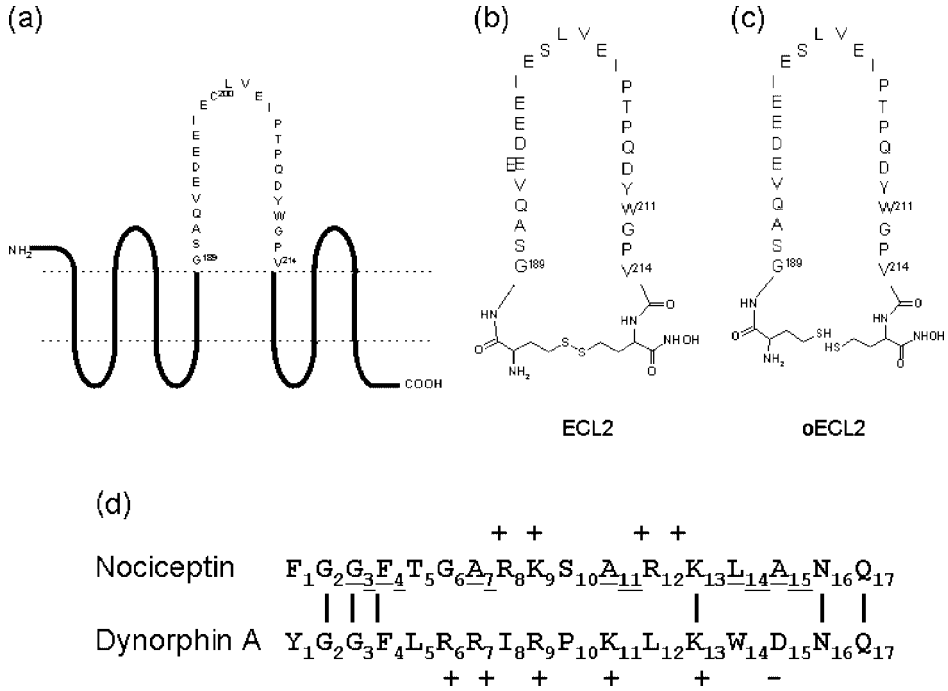

Figure 1 (a) Sequence of the second extracellular loop of the human Noc receptor and its mimicking peptide cyclic form (ECL2) (b). (c) oECL2 formed from ECL2 by reduction of the disulfide bond with TCEP (d) Sequence of Noc and of dynorphin A. The ^{15}N labeled amino acids used for NMR spectroscopy are underlined and identities between peptides are represented by a vertical line.

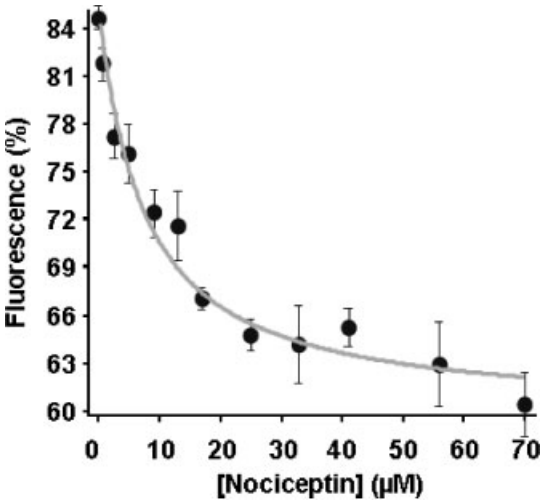

Figure 2 Plot of the relative fluorescence decreases at 356 nm as a function of total Noc concentration. The solid curve fits to Eqn (1) (Section on Material and Methods) and gives a K_d value of 7.2 ± 3.5 μM.

introduced in residues G_3 and F_4 belonging to the so-called 'message' of opioid peptides, and in residues A_7, A_{11}, A_{15} and L_{14} distributed throughout the remaining part of the peptide ('address') [43]. TOCSY, NOESY, and ^1H–^{15}N HSQC experiments were acquired in order to perform ^1H and ^{15}N sequential assignments in a standard manner.

The ^1H–^{15}N HSQC of Noc at 100 μM was recorded before and after the addition of equimolar concentration of ECL2 (Figure 3(a)). The spectra displayed the six expected cross peaks corresponding to the ^{15}N labeled amino acids. Addition of the cyclized ECL2 caused concentration-dependent chemical shift changes of particular ^{15}N labeled residues in Noc (Figure 3(c), (d)); this observation is indicative of a fast exchange on the ^1H and ^{15}N chemical shift time scale (i.e. a dissociation rate $k_{off} \gg 10$ Hz). The small spread and variation of ^1H and ^{15}N chemical shifts indicate that the interaction occurs without inducing a particular structuration of the ligand. HSQC experiments realized with the reduced form of ECL2, displayed no or less than 30% (in case of A_{11}) chemical shift modification when compared with Noc alone (Figure 3(b)). This result is important in the sense that it validates the use of a cyclic constrained loop as a model of the ECL2 loop within the entire receptor, as already observed by others [11]. The stoichiometry of the complex Noc–ECL2 was measured by titration experiments following the ^1H and ^{15}N chemical shift up to a 2 : 1 molar ratio (data not shown). Saturation was obtained for a molar ratio Noc : ECL2 1 : 1. ^1H and ^{15}N chemical shift variations plotted against the Noc : ECL2 ratio display saturation-like curves (Figure 3(c), (d)). The residues most sensitive to ECL2–Noc interaction are G_3, A_{11}, and L_{14} in the ^1H dimension, and F_4, A_7, A_{11}, and L_{14} in the ^{15}N dimension. Simultaneous fitting of all the binding isotherms for the ^{15}N and ^1H resonances [$\Delta\delta$ (^{15}N) > 0.01 ppm and $\Delta\delta$ (^1H) > 0.005 ppm], provided a dissociation constant (K_d) of 7 ± 3 μM. This K_d value is in agreement with the K_d

DOI: 10.1002/psc

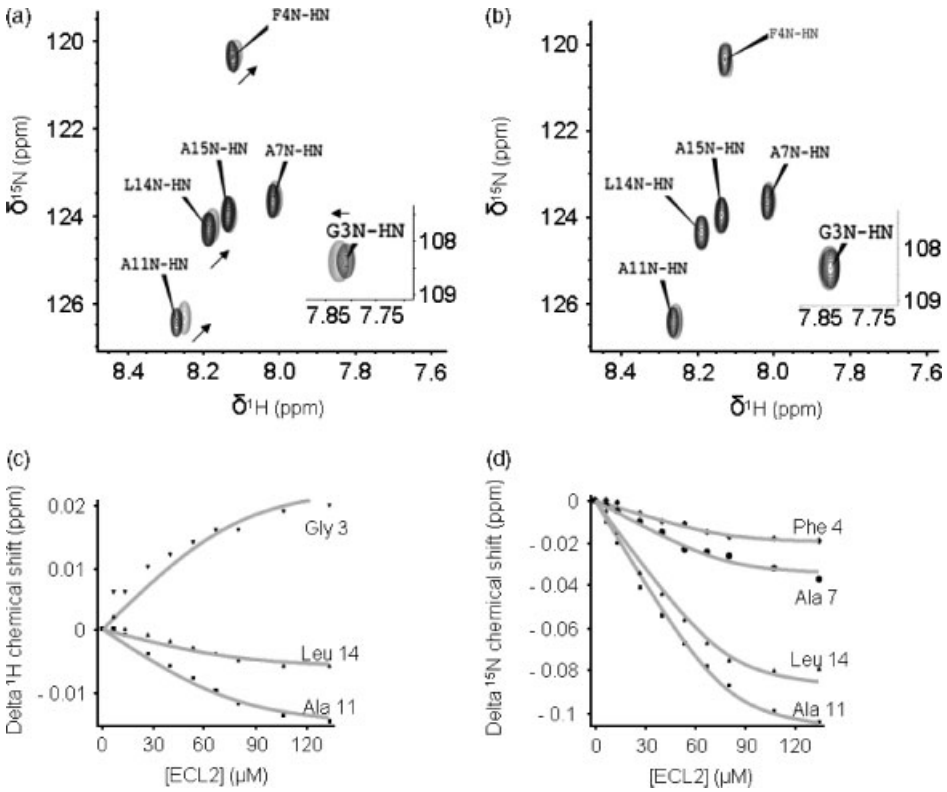

Figure 3 Overlays of HSQC $^{1}H-^{15}N$ spectrum of Noc alone (dark) or in the presence of cyclized (a) or opened (b) ECL2 (gray). The two peptides are in 10 mM phosphate buffer at pH 6 and at a concentration of 100 μM. To open the extracellular loop, 400 μM of TCEP has been added. Variations are more important when ECL2 is cyclized (Figure 1(b)) compared to the opened form (Figure 1(c)). Chemical shift ^{1}H (c) and ^{15}N (d) variations curves of Noc upon addition of ECL2. A K_d of 7 ± 3 μM was measured using the equation described in the Section on Materials and Methods.

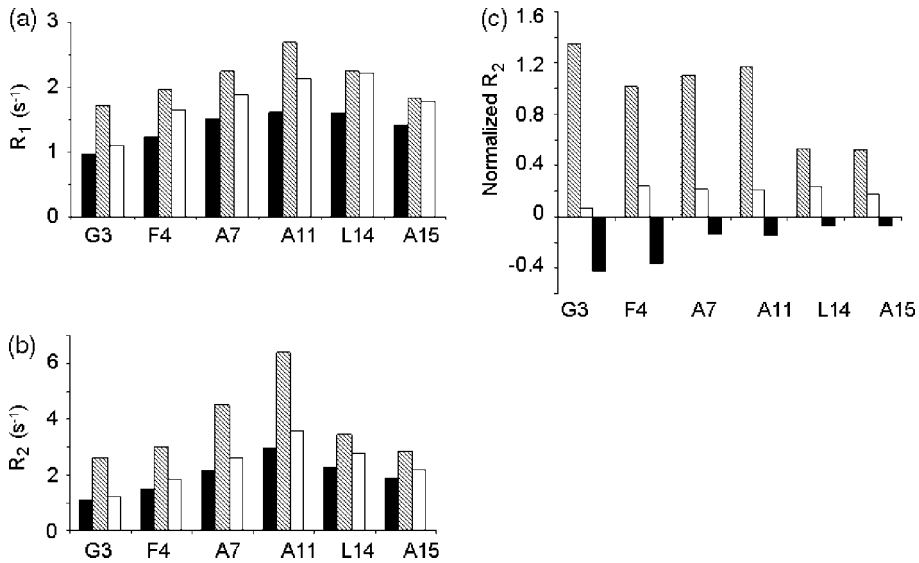

Figure 4 Relaxation parameters and $^{1}H-^{15}N$ NOE of free Noc (black), Noc–ECL2 complex (hashed), and Noc–oECL2 complex (white). ^{15}N R_1 rates (a), ^{15}N R_2 rates (b), and relative R_2 increase upon binding $(R_{2\text{complex Noc-ECL2}} - R_{2\text{Nocfree}})/R_{2\text{Nocfree}}$ (c).

determined by fluorescence spectroscopy. The major chemical shift variations concern both the 'address' part of the peptide (A_7, A_{11} and L_{14}) surrounded by the two RK basic motifs and the 'message' part of the peptide (G_3, F_4). G_3 ^{1}H chemical shift goes upfield, contrary to that of A_{11} and L_{14}. G_3 is close to F_1 and F_4 which, based on fluorescence spectroscopy results, were postulated to interact with the ECL2 tryptophan W_{211}. The ring

DOI: 10.1002/psc

current effect produced by this tryptophan may explain the observed chemical shift change of G_3 opposite to those observed for A_{11} and L_{14} and thus, this unusual NMR shift of G_3 is also in favor of proximity between Noc – G_3 and ECL2 – W_{211}. The necessity for a cyclic constrained loop for Noc binding suggests that the interaction is specific. This assumption is further supported by the fact that Dyn, another highly basic opioid peptide which has a very low affinity for NOP receptors, is inefficient in competing with ECL2–Noc interaction unless it is added in large excess (see below for a more detailed analysis of Dyn effects).

^{15}N Relaxation Time Evolutions upon Noc–ECL2 Interaction

To provide a more dynamic picture of the events associated with the formation of the Noc–ECL2 complex, ^{15}N relaxation experiments (T_1, T_2, and steady-state ^{1}H–^{15}N NOEs) were performed on the ^{15}N labeled Noc alone and in complex with the open and cyclic form of ECL2. R_1 and R_2 relaxation rates of free and bound Noc are plotted in Figure 4(a), (b). The R_1 and R_2 relaxation rates for the free Noc show a broad range of values that are larger in the middle compared to both ends. The R_1 and R_2 relaxation rates are similar for a given residue. These characteristics are expected for a rapidly tumbling peptide with unrestrained ends. In the presence of ECL2 (in ECL2–Noc complex 1 : 1 molar ratio), the relaxation rates increased, particularly R_2. The relative R_2 (defined as $[R_{2bound} - R_{2free}/R_{2free}]$) also increases upon binding (Figure 4(c)). These observations reveal that residues 14 and 15 on the *C*-terminus side are much less affected by the interaction with ECL2.

The R_2 variations upon binding can also be used to estimate the K_d. Indeed, in the fast exchange limit, the transverse relaxation rate R_2 is given by the simple average between bound and free states. R_{2bound} was estimated to be equal to 2.6 R_{2free} assuming a linear relation between R_2 and the molecular weight [44]. Within these approximations, the R_2 increase for residues 3, 4, 7, 11 corresponds to a K_d value of around 20 μM, in agreement with the K_d determined by fluorescence and NMR chemical shift variations.

The steady-state ^{1}H–^{15}N NOEs are negative for the free Noc as expected for a short peptide of 17 amino acids. Upon binding to the ECL2 loop, the ^{1}H–^{15}N NOEs increase to even become null for A_7 and L_{14} or positive for A_{11} due to the formation of a larger complex between Noc and ECL2 (data not shown). These observations confirm the formation of the complex and the importance of the amino acids near the two highly positive RK motifs.

The above NMR data, chemical shift variation, relaxation time, and steady-state ^{1}H–^{15}N NOE confirm an interaction between Noc and ECL2 in a micromolar range. Most importantly, the relaxation data (Figure 4(a), (b), (c)) measured after addition of 400 μM TCEP are similar to those of the free Noc. This again shows that the restraints to the ECL2's conformational space induced by cyclization are essential for specific recognition with Noc, thus making the cyclized ECL2 a significant model for the loop–Noc recognition in the entire receptor.

To investigate the specificity of the interaction, competition experiments with a closely related opioid peptide were performed. 1 Equivalent of Dyn is not sufficient to prevent Noc–ECL2 interaction, and 18 equivalents are required to compete with Noc. Thus ECL2 has more affinity for Noc than for Dyn by about one order of magnitude. R_2 relaxation rate is reversed for G_3 and F_4 and not for A_7, A_{11}, L_{14}, and A_{15} showing that Dyn competes more efficiently at the level of the *N*-terminus (Figure 5).

Mapping the Essential Residues Responsible for the Specific Interaction between Noc and ECL2

The interaction between Noc and ECL2 was further analyzed by observing the chemical shift perturbation by comparing the 2D ^{1}H spectra (TOCSY and NOESY) of Noc and ECL2 alone and the Noc–ECL2 complex. The proton resonance assignments were performed in the standard way for homonuclear NMR, i.e. identification of spin systems using the TOCSY spectra and sequential assignment using the NOESY spectra [45]. The complete proton resonance assignments for the Noc (Table 1), ECL2 (Table 2), and the complex were performed. The most significant Noc proton chemical shift variations upon ECL2 binding are observed on G_3 (already observed from the ^{15}N HSQC experiment), G_6, and Q_{17} NH and on the guanidinium protons of R_8 and R_{12}, which belong to the characteristic RK motif present twice in Noc. Interestingly, G_2 amide proton is not observable due to fast exchange in the free Noc peptide, while it became visible and could be assigned in the Noc–ECL2 complex. The same phenomenon was observed for side chain amine protons of K_9 and K_{13}. The significant reduction of the exchange rate of these labile protons indicates a long-lived interaction with the two lysines comprising the basic RK motif and G_2 which is part of the Noc *N*-terminal 'message'.

The ^{1}H and ^{13}C ECL2 chemical shift variations upon addition of Noc are summarized in Figure 6 and listed in Tables 2 and 3. The most important variations concern the central acidic region, particularly residues E_7, E_{10}, E_{12}, L_{14}, E_{16}. These residues are localized near the ECL2 S_{13} corresponding to cysteine 200 in the sequence of the human Noc receptor. This cysteine is known to form a disulfide bridge with cysteine 123 which is characteristic of the majority of the class A GPCRs and is essential for their activities [46]. In the same central acidic region, the β-carbon resonances of glutamate and aspartate are shifted downfield upon Noc addition

DOI: 10.1002/psc

Table 1 Proton resonance assignment (in ppm) for the nociceptin and in complex with ECL2 in parentheses

Residues	HN	Hα	Hβ	Hγ	Hδ	Hε	Hζ	Hη
G2	ND (8.471)	ND (3.675)	—	—	—	—	—	—
G3	7.808 (7.823)	3.645 (3.649)	—	—	—	—	—	—
F4	8.129 (8.134)	4.503 (4.506)	2.863 (2.864)	—	—	—	—	—
T5	8.104 (8.103)	4.079 (4.086)	3.986 (3.985)	0.941 (0.941)	—	—	—	—
G6	7.573 (7.559)	3.641 (3.639)	—	—	—	—	—	—
A7	8.019 (8.019)	4.072 (4.075)	1.144 (1.143)	—	—	—	—	—
R8	8.217 (8.217)	4.065 (4.061)	1.537 (1.535)	1.394 (1.396)	2.939 (2.934)	ND (ND)	—	6.974 (6.957)
K9	8.269 (8.272)	4.069 (4.072)	1.592/1.513 (1.588/1.52)	1.198 (1.198)	1.449 (1.451)	2.758 (2.759)	ND (7.352)	—
S10	8.198 (8.192)	4.182 (4.182)	3.622 (3.620)	—	—	—	—	—
A11	8.265 (8.260)	4.093 (4.100)	1.159 (1.158)	—	—	—	—	—
R12	8.105 (8.101)	4.033 (4.035)	1.537 (1.531)	1.386 (1.386)	2.957 (2.955)	ND (ND)	—	7.004 (6.988)
K13	8.269 (8.272)	4.069 (4.072)	1.592/1.513 (1.588/1.52)	1.198 (1.198)	1.449 (1.451)	2.758 (2.759)	ND (7.352)	—
L14	8.191 (8.193)	4.116 (4.125)	1.376 (1.376)	1.400 (1.401)	0.638/0.696 (0.636/0.696)	—	—	—
A15	8.138 (8.141)	4.057 (4.062)	1.162 (1.162)	—	—	—	—	—
N16	8.252 (8.252)	4.411 (4.410)	2.598 (2.598)	—	6.723/7.467 (6.723/7.467)	—	—	—
Q17	7.655 (7.667)	3.937 (3.943)	1.708/1.894 (1.709/1.896)	2.043 (2.048)	—	6.673/7.385 (6.675/7.383)	—	—

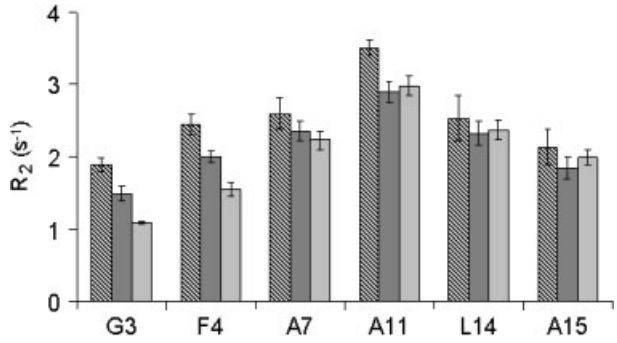

Figure 5 Relaxation parameter (R_2) of the preformed complex Noc–ECL2 (hashed) decreases upon competition with 0.3 (gray) and 18 (light gray) equivalents of Dyn.

(Figure 6(b)). This systematic downfield shift of acidic residues is a clear indication of their interaction with positively charged RK residues of Noc.

To further characterize the electrostatic nature of the interaction, the effect of sodium chloride was visualized by HSQC $^{1}H-^{15}N$. Upon addition of NaCl, the chemical shift variations observed on A_{11} and L_{14} are reversed, only the G3 variation remains (data not shown). This shows that while the *C*-terminal interaction is mostly of an electrostatic nature, the *N*-terminus interaction energy contains a nonelectrostatic component.

It is interesting to note that the interaction between Noc and ECL2 is perturbed by NaCl or Dyn in different ways, NaCl suppressing more effectively interaction due to the central part of Noc, while Dyn competes at the *N*-terminal part, more hydrophobic (see above, ^{15}N R_2 relaxation experiments in Figure 5).

DISCUSSION

In this study the interaction of Noc and an extracellular loop mimicking peptide (ECL2) was examined in solution by fluorescence and NMR spectroscopy. The structure activity relationship in the Noc–receptor system and the ligand selectivity recognition indicate that the second extracellular loop plays a key role in the binding and, thus, the activity of the receptor [26]. The purpose of this study was to validate and define the interaction of the second extracellular NOP loop with Noc and the role of this interaction in terms of selectivity to other similar opioid ligands like Dyn. Noc was shown previously to be unstructured in aqueous solution [47,48]. Our data confirm this conclusion for Noc alone and also complexed with ECL2 of its receptor. Several experimental conditions using surfactants or organic solvents [47–49] have previously been used in order to stabilize Noc conformations giving mixed results. In a first approach, we performed our studies in aqueous solution near the physiological pH. The fact that we could demonstrate saturable binding between Noc and cyclized loop ECL2, prompted us to pursue

DOI: 10.1002/psc

Table 2 Proton resonance assignment (in ppm) for the ECL2 and in complex with nociceptin in parentheses

Residues	HN	Hα	Hβ	Hγ	Hδ	Hε	HZ	HH
Hc1	ND (ND)	3.955 (3.947)	2.085 (2.079)	2.574 (2.565)	—	—	—	—
G2	8.623 (8.651)	3.847 (3.844)	—	—	—	—	—	—
S3	8.252 (8.273)	4.256 (4.263)	3.670 (3.671)	—	—	—	—	—
A4	8.27 (8.256)	4.127 (4.108)	1.185 (1.19)	—	—	—	—	—
Q5	8.136 (8.173)	4.131 (4.146)	1.781/1.883 (1.775/1.889)	2.141 (2.138)	—	6.701/7.397 (6.695/7.433)	—	—
V6	8.002 (8.038)	3.893 (3.921)	1.866 (1.871)	0.727 (0.729)	—	—	—	—
E7	8.337 (8.424)	4.124 (4.099)	1.761/1.887 (1.734/1.869)	2.171 (2.099)	—	—	—	—
D8	8.213 (8.181)	4.408 (4.375)	2.537/2.616 (2.450/2.549)	—	—	—	—	—
E9	8.178 (8.179)	4.099 (4.063)	ND (1.763)	ND (2.120)	—	—	—	—
E10	8.178 (8.267)	4.099 (4.098)	ND (1.782/1.873)	ND (2.058/2.123)	—	—	—	—
I11	7.885 (7.924)	3.928 (3.941)	1.699 (1.684)	1.287/1.005/0.71 (0.99/1.27/0.71)	0.71 (0.71)	—	—	—
E12	8.239 (8.322)	4.121 (4.082)	1.798/1.897 (1.764/1.856)	2.208 (2.106)	—	—	—	—
S13	8.055 (8.110)	4.213 (4.231)	3.677 (3.662)	—	—	—	—	—
L14	8.038 (8.131)	4.180 (4.196)	1.426 (1.434)	1.496 (1.434)	0.671/0.724 (0.658/0.753)	—	—	—
V15	7.773 (7.806)	3.915 (3.917)	1.871 (1.861)	0.719 (0.718)	—	—	—	—
E16	8.148 (8.214)	4.136 (4.095)	1.747 (1.714/1.796)	2.146 (1.986/2.075)	—	—	—	—
I17	8.034 (8.049)	4.273 (4.271)	1.671 (1.669)	1.294/0.956/0.734 (1.298/0.953/0.731)	0.648 (0.644)	—	—	—
P18		4.273 (4.266)	1.680/2.063 (1.673/2.063)	1.776 (1.783)	3.493/3.673 (3.495/3.662)	—	—	—
T19	8.120 (8.151)	4.384 (4.365)	3.973 (3.947)	1.028 (1.024)	—	—	—	—
P20		4.164 (4.171)	1.708/2.123 (1.732/2.120)	1.794 (1.796)	3.457/3.673 (3.442/3.662)	—	—	—
Q21	8.226 (8.242)	3.966 (3.976)	1.717/1.804 (1.712/1.806)	2.112 (2.120)	—	6.701/7.353 (6.698/7.361)	—	—
D22	8.067 (8.083)	4.315 (4.298)	2.414 (2.373)	—	—	—	—	—
Y23	7.630 (7.633)	4.190 (4.184)	2.549/2.657 (2.535/2.659)	—	6.685 (6.683)	6.495 (6.492)	—	—
W24	7.804 (7.821)	4.458 (4.451)	2.922/3.119 (2.914/3.117)	—	7.005 (7.003)	7.392/9.934 (7.399/9.945)	6.947/7.285 (6.948/7.286)	7.032 (7.035)
G25	7.123 (7.087)	3.759 (3.747)	—	—	—	—	—	—
P26		4.250 (4.244)	1.726/2.073 (1.720/2.071)	1.813 (1.809)	3.34/3.395 (3.348/3.390)	—	—	—
V27	8.078 (8.095)	3.843 (3.846)	1.848 (1.854)	0.747 (0.738)	—	—	—	—
Hc28	8.351 (8.357)	4.21 (4.207)	1.896/1.942 (1.889/1.948)	2.487/2.563 (2.475/2.566)	—	—	—	—

DOI: 10.1002/psc

Table 3 Carbon resonance assignment (in ppm) for the ECL2 and in complex with nociceptin in parentheses

Residues	Cα	Cβ	Cγ	Cδ	Cε	Cζ2	Cζ3	Cη
Hc1	52.0 (52.1)	30.0 (30.1)	31.6 (31.6)	—	—	—	—	—
G2	42.3 (42.4)	—	—	—	—	—	—	—
S3	55.6 (55.5)	61.0 (61.1)	—	—	—	—	—	—
A4	49.9 (49.7)	16.3 (16.5)	—	—	—	—	—	—
Q5	53.2 (52.9)	26.5 (26.7)	31.1 (31.0)	—	—	—	—	—
V6	59.7 (59.5)	29.9 (30.0)	—	—	—	—	—	—
E7	53.6 (53.6)	26.5 (27.2)	31.4 (33.0)	—	—	—	—	—
D8	51.4 (51.7)	37.1 (38.1)	—	—	—	—	—	—
E9	53.7 (53.9	26.5 (27.3)	31.4 (33.0)	—	—	—	—	—
E10	53.7 (53.6)	26.5 (27.4)	31.4 (33.0)	—	—	—	—	—
I11	58.7 (58.6)	35.8 (5.9)	24.6 (24.5)	—	—	—	—	—
E12	53.7 (53.7)	26.5 (27.2)	31.4 (33.0)	—	—	—	—	—
S13	55.6 (55.5)	61.0 (61.0)	—	—	—	—	—	—
L14	55.7 (55.5)	39.4 (39.6)	24.1 (26.3)	—	—	—	—	—
V15	59.6 (59.5)	29.9 (30.0)	—	—	—	—	—	—
E16	53.2 (53.6)	26.5 (27.4)	31.2 (33.1)	—	—	—	—	—
I17	55.6 (55.6)	35.8 (35.9)	24.1 (24.1)	—	—	—	—	—
P18	60.3 (60.3)	29.4 (29.4)	24.6 (24.6)	48.3 (48.3)	—	—	—	—
T19	57.0 (57.1)	67.0 (66.9)	18.8 (18.8)	—	—	—	—	—
P20	60.8 (60.7)	29.4 (29.4)	24.5 (24.5)	48.2 (48.2)	—	—	—	—
Q21	53.6 (53.6)	26.5 (26.5)	31.0 (30.9)	—	—	—	—	—
D22	51.1 (51.4)	37.3 (37.9)	—	—	—	—	—	—
Y23	52.6 (52.5)	36.2 (36.2)	—	130.3 (130.3)	115.3 (115.3)	—	—	—
W24	54.0 (54.0)	26.9 (26.9)	—	124.5 (124.5)	118.2 (118.2)	111.8 (111.8)	119.2 (119.2)	121.8 (121.8)
G25	41.9 (41.9)	—	—	—	—	—	—	—
P26	60.3 (60.3)	29.4 (29.4)	24.5 (24.5)	46.9 (46.9)	—	—	—	—
V27	59.8 (59.8)	29.9 (30.0)	—	—	—	—	—	—
Hc28	55.6 (55.5)	29.9 (29.8)	33.1 (33.1)	—	—	—	—	—

DOI: 10.1002/psc

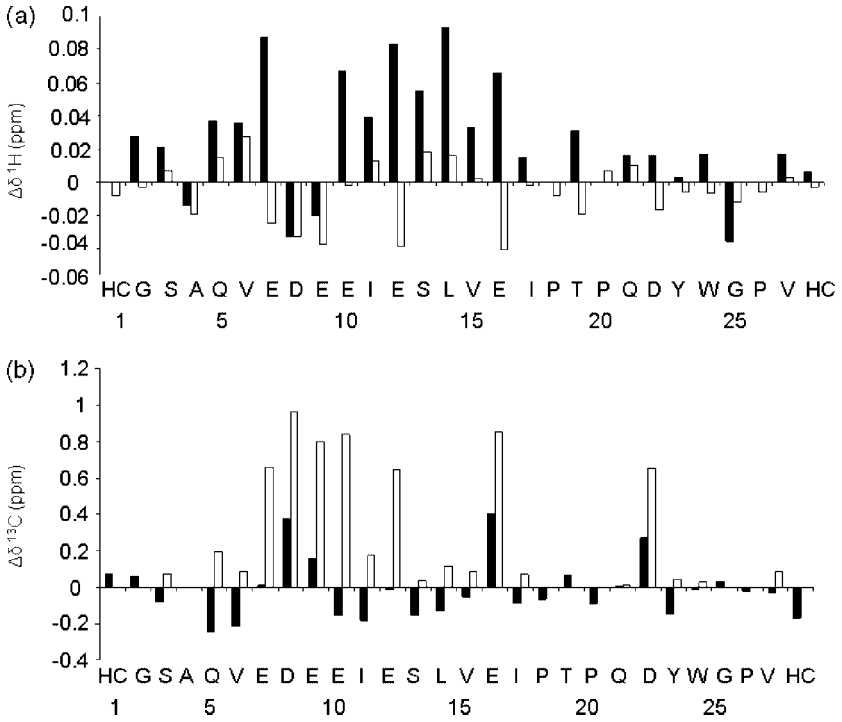

Figure 6 ^{1}H [HN (black) and HA (gray)] (a) and ^{13}C [Cα (black) and Cβ (gray)] (b) chemical shift variation between free Noc and the complex Noc–ECL2.

the NMR characterization of the ligand–loop complex under these conditions.

Owing to the lack of structural information of this GPCR, an alternative approach to characterize the molecular interaction between a ligand and its receptor is to use peptide fragments mimicking parts of these large membrane proteins. The model used to mimic the extracellular loop of the Noc receptor is a linear peptide composed of the whole sequence of the secondary extracellular loop containing homocysteines at both ends. The intramolecular oxidative formation of a disulfide bridge constrains the distance of the *N*- and *C*-termini to a distance of 8–12 ´Å and still allows a large flexibility to mimic the dynamics occurring between the transmembrane helices 4 and 5. To validate this cyclic peptidic fragment approach, the binding constant between Noc and ECL2 was measured using fluorescence, NMR relaxation rates, and chemical shift variations. Both techniques used allowed us to measure a K_d of 7 ± 3 μM. The reduction of the disulfide bridge to form a linear peptide dramatically decreased the K_d ($K_d > 1$ mM), proving that this interaction is conformation dependent. The cyclic constraint contributed to limit the conformational space of this peptide and therefore to provide the required conformation of essential residues of ECL2 implicated in the interaction with Noc. Furthermore, competition experiments with Dyn, a closely related opioid peptide specific of the KOP1 receptor, indicate that ECL2 has an intrinsic capability to discriminate between Dyn and Noc. This drives to a difference in affinity of one order of magnitude.

In the conditions used for NMR studies, structural information about Noc and ECL2 alone and the complex are poor, in particular, in NOESY experiments. The size and internal dynamics of this system prevented us from defining precisely a 3D structure of the Noc–ECL2 complex. Nevertheless, chemical shift mapping and ^{15}N relaxation analyses revealed a number of specific components in this interaction. The NMR relaxation data, notably the transverse relaxation measurement showed us that this interaction involves essentially the *N*-terminal and the central part of Noc. This peptidic sequence contains the two basic RK motifs characteristic of this neuropeptide and the FGGF sequence, so-called message sequence, similar to the opioid sequence YGGF found in Dyn A, β endorphin, and enkephalins. These results are in agreement with the binding constant measurement made between the whole receptor and the truncated Noc 1–13 [28,43]. The deletion of the last four *C*-terminal amino acids (L_{14}-A_{15}-N_{16}-Q_{17}) from the Noc results in a loss of only 1/30th affinity compared to the parent Noc, indicating that the most specific interactions occur principally with the peptide sequence Noc 1–13. Deletion or substitutions of the two basic motifs render the peptide totally inactive or dramatically decrease the affinity of the Noc, proving that the two RK motifs are involved in the specific interaction with the NOP receptor [50,51]. This ionic interaction of Noc with ECL2 involves the guanidinium groups of two arginines that undergo

DOI: 10.1002/psc

a chemical shift variation in the presence of ECL2 and the amine protons of the radical chain of two lysines characterized by a chemical exchange rate modification, when the Noc interacts with ECL2. Both basic motifs are required for a specific interaction of Noc with its receptor. Furthermore, the fact that all the acidic area on ECL2, highly conserved in all species, is also affected suggests an ionic interaction between this part of ECL2 and the central basic part of Noc. Perturbing the interaction by increasing the ionic strength of the solution by adding NaCl canceled the chemical shift variation of the basic part of Noc. Interestingly, the interaction between Noc and ECL2 involves a second set of physical properties. Chemical shift variations of the *N*-terminal part of Noc show a saturable effect upon addition of ECL2, which is not reversed by NaCl addition. The interaction is supported by an increase in R_2, which is sensible to Dyn competition. Based on the results obtained, it is thus reasonable to hypothesize that the binding of Noc to ECL2 involves two types of interactions: an ionic one between its basic motifs and the acidic residues of ECL2 and a hydrophobic one concerning the *N*-terminal part of Noc. This second interaction site is supported by the fluorescence-quenching phenomena observed during the complex formation that could result from a hydrophobic interaction between the aromatic ring of the phenylalanines present in the message address of Noc and the tryptophane of the ECL2. Site-directed mutagenesis and molecular modeling studies have suggested that the binding site for the Noc *N*-terminal message sequence is located deeper within the transmembrane domain of the receptor [5]. In the context of a full size receptor, the interaction between FGGF and the aromatic region of ECL2 is proposed to be only transient, representing a low-affinity intermediate state in the binding mechanism.

In summary, the extracellular loop of the NOP receptor plays a crucial role in ligand binding and selectivity. A mimicking peptide of the extracellular loop can bind the Noc with an affinity constant of about 7 μM. This interaction involves two kinds of interactions: an ionic interaction between the two basic motifs (RK) characteristic of the Noc ligand and the acidic residues of the second loop, but also a hydrophobic one implicating the *N*-terminal message sequence with a specific aromatic cluster found at the beginning of the transmembrane helix 5. These data reinforce the hypothesis that ECL2 participates in selectivity, by orienting the neuropeptide to prepare its final recognition with a nanomolar affinity by a binding site localized in the helices bundle core of this GPCR.

Acknowledgements

This work was realized on NMR spectrometers financed by CNRS, the 'Région Midi-Pyrénées', and European structural funds (FEDER). The studies were supported by the French research ministry, CNRS, Université Paul Sabatier, the Région Midi-Pyrénées, and European structural funds. We would like to thank Dr Christopher Topham for the helpful discussion about the design of the mimicking peptide ECL2 used for this study.

REFERENCES

1. Chiou LC, Liao YY, Fan PC, Kuo PH, Wang CH, Riemer C, Prinssen EP. Nociceptin/orphanin FQ peptide receptors: pharmacology and clinical implications. *Curr. Drug Targets.* 2007; **8**: 117–135.
2. Meunier J-C. The potential therapeutic value of nociceptin receptor agonists and antagonists. *Expert Opin. Ther. Pat.* 2000; **10**: 371–388.
3. Meunier J, Mouledous L, Topham CM. The nociceptin (ORL1) receptor: molecular cloning and functional architecture. *Peptides* 2000; **21**: 893–900.
4. Philip AE, Poupaert JH, McCurdy CR. Opioid receptor-like 1 (ORL1) molecular 'road map' to understanding ligand interaction and selectivity. *Curr. Top. Med. Chem.* 2005; **5**: 325–340.
5. Topham CM, Mouledous L, Poda G, Maigret B, Meunier JC. Molecular modelling of the ORL1 receptor and its complex with nociceptin. *Protein Eng.* 1998; **11**: 1163–1179.
6. Metzger TG, Ferguson DM. On the role of extracellular loops of opioid receptors in conferring ligand selectivity. *FEBS Lett.* 1995; **375**: 1–4.
7. Palczewski K, Kumasaka T, Hori T, Behnke CA, Motoshima H, Fox BA, Le Trong I, Teller DC, Okada T, Stenkamp RE, Yamamoto M, Miyano M. Crystal structure of rhodopsin: a G protein-coupled receptor. *Science* 2000; **289**: 739–745.
8. Rasmussen SGF, Choi HJ, Rosenbaum DM, Kobilka TS, Thian FS, Edwards PC, Burghammer M, Ratnala VRP, Sanishvili R, Fischetti RF, Schertler GFX, Weis WI, Kobilka BK. Crystal structure of the human beta(2) adrenergic G-protein-coupled receptor. *Nature* 2007; **450**: 383–387.
9. Cherezov V, Rosenbaum DM, Hanson MA, Rasmussen SGF, Thian FS, Kobilka TS, Choi HJ, Kuhn P, Weis WI, Kobilka BK, Stevens RC. High-resolution crystal structure of an engineered human beta(2)-adrenergic G protein-coupled receptor. *Science* 2007; **318**: 1258–1265.
10. Sarramegna V, Talmont R, Demange P, Milon A. Heterologous expression of G-protein-coupled receptors: comparison of expression systems from the standpoint of large-scale production and purification. *Cell. Mol. Life Sci.* 2003; **60**: 1529–1546.
11. Yeagle PL, Albert AD. G-protein coupled receptor structure. *Biochim. Biophys. Acta* 2007; **1768**: 530–537.
12. Katragadda M, Alderfer JL, Yeagle PL. Solution structure of the loops of bacteriorhodopsin closely resembles the crystal structure. *Biochim. Biophys. Acta* 2000; **1466**: 1–6.
13. Ruan KH, So SP, Wu J, Li D, Huang A, Kung J. Solution structure of the second extracellular loop of human thromboxane A2 receptor. *Biochemistry* 2001; **40**: 275–280.
14. Zhang L, DeHaven RN, Goodman M. NMR and modeling studies of a synthetic extracellular loop II of the kappa opioid receptor in a DPC micelle. *Biochemistry* 2002; **41**: 61–68.
15. Petry R, Craik D, Haaima G, Fromme B, Klump H, Kiefer W, Palm D, Millar R. Secondary structure of the third extracellular loop responsible for ligand selectivity of a mammalian gonadotropin-releasing hormone receptor. *J. Med. Chem.* 2002; **45**: 1026–1034.
16. Nicastro G, Peri F, Franzoni L, de Chiara C, Sartor G, Spisni A. Conformational features of a synthetic model of the first

extracellular loop of the angiotensin II AT1A receptor. *J. Pept. Sci.* 2003; **9**: 229–243.
17. Ruan KH, Wu J, So SP, Jenkins LA. Evidence of the residues involved in ligand recognition in the second extracellular loop of the prostacyclin receptor characterized by high resolution 2D NMR techniques. *Arch. Biochem. Biophys.* 2003; **418**: 25–33.
18. Ulfers AL, Piserchio A, Mierke DF. Extracellular domains of the neurokinin-1 receptor: structural characterization and interactions with substance P. *Biopolymers* 2002; **66**: 339–349.
19. Giragossian C, Mierke DF. Determination of ligand-receptor interactions of cholecystokinin by nuclear magnetic resonance. *Life Sci.* 2003; **73**: 705–713.
20. Fadhil I, Schmidt R, Walpole C, Carpenter KA. Exploring deltorphin II binding to the third extracellular loop of the delta-opioid receptor. *J. Biol. Chem.* 2004; **279**: 21069–21077.
21. Pham TCT, Kriwacki RW, Parrill AL. Peptide design and structural characterization of a GPCR loop mimetic. *Biopolymers* 2007; **86**: 298–310.
22. Ye JP, Kohli LL, Stone MJ. Characterization of binding between the chemokine eotaxin and peptides derived from the chemokine receptor CCR3. *J. Biol. Chem.* 2000; **275**: 27250–27257.
23. So SP, Wu JX, Huang GX, Huang AM, Li DW, Ruan KH. Identification of residues important for ligand binding of thromboxane A(2) receptor in the second extracellular loop using the NMR experiment-guided mutagenesis approach. *J. Biol. Chem.* 2003; **278**: 10922–10927.
24. Amodeo P, Guerrini R, Picone D, Salvadori S, Spadaccini R, Tancredi T, Temussi PA. Solution structure of nociceptin peptides. *J. Pept. Sci.* 2002; **8**: 497–509.
25. Meunier JC, Mollereau C, Toll L, Suaudeau C, Moisand C, Alvinerie P, Butour JL, Guillemot JC, Ferrara P, Monsarrat B, Mazarguil H, Vassart G, Parmentier M, Constentin J. Isolation and structure of the endogenous agonist of opioid receptor-like ORL1 receptor [see comments]. *Nature* 1995; **377**: 532–535.
26. Mollereau C, Mouledous L, Lapalu S, Cambois G, Moisand C, Butour JL, Meunier JC. Distinct mechanisms for activation of the opioid receptor-like 1 and kappa-opioid receptors by nociceptin and dynorphin A. *Mol. Pharmacol.* 1999; **55**: 324–331.
27. Lapalu S, Moisand C, Mazarguil H, Cambois G, Mollereau C, Meunier JC. Comparison of the structure-activity relationships of nociceptin and dynorphin A using chimeric peptides. *FEBS Lett.* 1997; **417**: 333–336.
28. Butour JL, Moisand C, Mazarguil H, Mollereau C, Meunier JC. Recognition and activation of the opioid receptor-like ORL 1 receptor by nociceptin, nociceptin analogs and opioids. *Eur. J. Pharmacol.* 1997; **321**: 97–103.
29. Chavkin C, Goldstein A. Specific receptor for the opioid peptide dynorphin: structure–activity relationships. *Proc. Natl. Acad. Sci. U.S.A.* 1981; **78**: 6543–6547.
30. Mansour A, Hoversten MT, Taylor LP, Watson SJ, Akil H. The cloned mu, delta and kappa receptors and their endogenous ligands: evidence for two opioid peptide recognition cores. *Brain Res.* 1995; **700**: 89–98.
31. Mouledous L, Topham CM, Mazarguil H, Meunier JC. Direct identification of a peptide binding region in the opioid receptor-like 1 receptor by photoaffinity labeling with [Bpa(10),Tyr(14)]nociceptin. *J. Biol. Chem.* 2000; **275**: 29268–29274.
32. Klco JM, Wiegand CB, Narzinski K, Baranski TJ. Essential role for the second extracellular loop in C5a receptor activation. *Nat. Struct. Mol. Biol.* 2005; **12**: 320–326.
33. Ott TR, Troskie BE, Roeske RW, Illing N, Flanagan CA, Millar RP. Two mutations in extracellular loop 2 of the human GnRH receptor convert an antagonist to an agonist. *Mol. Endocrinol.* 2002; **16**: 1079–1088.
34. Vertongen P, Solano RM, Juarranz MG, Perret J, Waelbroeck M, Robberecht P. Proline residue 280 in the second extracellular loop (EC2) of the VPAC2 receptor is essential for the receptor structure. *Peptides* 2001; **22**: 1363–1370.
35. Baneres JL, Mesnier D, Martin A, Joubert L, Dumuis A, Bockaert J. Molecular characterization of a purified 5-HT4 receptor: a structural basis for drug efficacy. *J. Biol. Chem.* 2005; **280**: 20253–20260.
36. Piotto M, Saudek V, Sklenar V. Gradient-tailored excitation for single-quantum NMR spectroscopy of aqueous solutions. *J. Biomol. NMR* 1992; **2**: 661–665.
37. Hwang TL, Shaka AJ. Water suppression that works. Excitation sculpting using arbitrary Wave-forms and Pulsed-field gradients. *J. Magn. Reson., Ser. A* 1995; **112**: 275–279.
38. Shaka AJ, Lee CJ, Pines A. Iterative schemes for bilinear operators; application to spin decoupling. *J. Magn. Reson.* 1988; **77**: 274–293.
39. Delaglio F, Grzesiek S, Vuister GW, Zhu G, Pfeifer J, Bax A. NMRPIPE – a multidimensional spectral processing system based on Unix pipes. *J. Biomol. NMR* 1995; **6**: 277–293.
40. Farrow NA, Muhandiram R, Singer AU, Pascal SM, Kay CM, Gish G, Shoelson SE, Pawson T, Formankay JD, Kay LE. Backbone dynamics of the free and a phosphopeptide-complexed SRC homology-2 domain studied by N-15 NMR relaxation. *Biochemistry* 1994; **33**: 5984–6003.
41. Ross JB, Szabo AG, Hogue CW. Enhancement of protein spectra with tryptophan analogs: fluorescence spectroscopy of protein-protein and protein-nucleic acid interactions. *Methods Enzymol.* 1997; **278**: 151–190.
42. Adams PD, Chen Y, Ma K, Zagorski MG, Sonnichsen FD, McLaughlin ML, Barkley MD. Intramolecular quenching of tryptophan fluorescence by the peptide bond in cyclic hexapeptides. *J. Am. Chem. Soc.* 2002; **124**: 9278–9286.
43. Guerrini R, Calo G, Rizzi A, Bianchi C, Lazarus LH, Salvadori S, Temussi PA, Regoli D. Address and message sequences for the nociceptin receptor: a structure-activity study of nociceptin-(1–13)-peptide amide. *J. Med. Chem.* 1997; **40**: 1789–1793.
44. Ryabov YE, Geraghty C, Varshney A, Fushman D. An efficient computational method for predicting rotational diffusion tensors of globular proteins using an ellipsoid representation. *J. Am. Chem. Soc.* 2006; **128**: 15432–15444.
45. Wuthrich K. *NMR of Proteins and Nucleic Acid used*. John Wiley and Sons: New York, 1986.
46. Bockaert J, Pin JP. Molecular tinkering of G protein-coupled receptors: an evolutionary success. *EMBO J.* 1999; **18**: 1723–1729.
47. Klaudel L, Legowska A, Brzozowski K, Silberring J, Wojcik J. Solution conformational study of nociceptin and its 1–13 and 1–11 fragments using circular dichroism and two-dimensional NMR in conjunction with theoretical conformational analysis. *J. Pept. Sci.* 2004; **10**: 678–690.
48. Orsini MJ, Nesmelova I, Young HC, Hargittai B, Beavers MP, Liu J, Connolly PJ, Middleton SA, Mayo KH. The nociceptin pharmacophore site for opioid receptor binding derived from the NMR structure and bioactivity relationships. *J. Biol. Chem.* 2005; **280**: 8134–8142.
49. Salvadori S, Picone D, Tancredi T, Guerrini R, Spadaccini R, Lazarus LH, Regoli D, Temussi PA. Solution conformation of nociceptin. *Biochem. Biophys. Res. Commun.* 1997; **233**: 640–643.
50. Reinscheid RK, Ardati A, Monsma FJ, Civelli O. Structure-activity relationship studies on the novel neuropeptide orphanin FQ. *J. Biol. Chem.* 1996; **271**: 14163–14168.
51. Dooley CT, Houghten RA. Orphanin FQ: receptor binding and analog structure activity relationships in rat brain. *Life Sci.* 1996; **59**: PL23–PL29.

DOI: 10.1002/psc